Environmental Science and Pollution Research
https://doi.org/10.1007/s11356-022-23446-2

RESEARCH ARTICLE

Optimization and kinetic modeling of phosphate recovery as struvite by electrocoagulation from source-separated urine

Alisha Zaffar[1] · Nageshwari Krishnamoorthy[1] · Nahaarjun Nagaraj[1] · Sivaraman Jayaraman[1] · Balasubramanian Paramasivan[1]

Received: 15 March 2022 / Accepted: 30 September 2022
© The Author(s), under exclusive licence to Springer-Verlag GmbH Germany, part of Springer Nature 2022

Abstract

Phosphorus recovery is indispensable due to the rapid depletion of its natural reserves and excessive utility in agriculture. Though human urine has high nutrient content including phosphate, nitrogen and potassium; direct use as a fertilizer is restricted due to hygienic, environmental, social and ethical issues. To overcome these limitations, the nutrients are precipitated by the external addition of magnesium (Mg) to form a slow-releasing fertilizer called struvite. The present study aims to maximize phosphate recovery through optimizing struvite production by an emerging electrocoagulation technique. A maximum of 95% phosphate recovery was achieved using inter-electrode distance of 0.5 cm, 2 A current from undiluted urine using Mg–Mg electrodes in a reaction time of 30 min. Further, kinetic modeling of phosphate recovery through electrocoagulation was conducted to comprehend the intended mechanism through the order of kinetics. The results revealed that the data best correlated with first-order kinetics with a correlation coefficient of 0.95. Electrocoagulation improved the supernatant quality by reducing the ion concentrations other than phosphate (30–50%), salinity (40–45%), and microbial population (99%). Qualitative assessment of the precipitate through sophisticated analysis further confirmed the presence of struvite crystals.

Keywords Struvite · Electrocoagulation · Human urine · Phosphorus · Resource recovery

Introduction

Phosphorus is a fundamental element required to produce crops. It is absorbed by plants through soil in the form of phosphates and gets incorporated in the food chain. Population explosion and climate change have deteriorated agricultural fields' innateness, reducing soil fertility. To tackle these pressing issues and food supply demands, phosphate rocks have been extensively mined for commercial fertilizer production. This resource is non-renewable and is expected to exhaust by 2092 if an alternative strategy for recovery is not devised (García et al. 2013). Reclamation of nutrients from wastewaters has gained the limelight in terms of phosphate recovery and alleviating eutrophication. The researchers have used various remediation methods for waste and wastewater phosphate removal, including membrane filtration, electrochemical precipitation, ion exchange, chemical, biological, coagulation-flocculation, electro-catalytical, electrocoagulation, fuel cells, and other hybrid methods (Jaafari et al. 2019; Naghipour et al. 2020). Most of these processes were studied from a reaction mechanism point of view rather than economical or commercialization aspect. Also, the non-implementable design complicating the process of nutrient recovery poses as a major drawback while scaling up the process for real-time scenarios (Peng et al. 2018).

Struvite or magnesium ammonium phosphate (MAP), a phosphate-rich fertilizer produced by forced precipitation of nutrients, has become a novel and sustainable approach for resource recovery from wastewaters (Zhang et al. 2018). The wastewater source can be landfill leachate (Shu et al. 2016), anaerobic digesters (Lee et al. 2015), human urine (Hug and Udert 2013), municipal wastewater (Jabr et al. 2019), or cooking wastewater (Huang et al. 2016). Being a slow-release fertilizer, frequent application of struvite on the agricultural field can be avoided, reducing the cost incurred on soil reclamation over a period and the pressure of phosphorus

Responsible Editor: Angeles Blanco

✉ Balasubramanian Paramasivan
biobala@nitrkl.ac.in

[1] Department of Biotechnology & Medical Engineering, National Institute of Technology, Rourkela, Odisha 769008, India

Published online: 18 October 2022

rock depletion (Lin et al. 2015; Yetilmezsoy et al. 2017). Struvite recovery can also be used as pre-treatment or post-treatment technology to enhance wastewater treatment (Tian et al. 2016). Urine, also known as liquid fertilizer, is a potent alternative for phosphorus and other nutrients essential for plant growth. Though urine accounts for only 1% of the total wastewater volume, it contributes to more than 50% of the phosphorus and 90% of ammonium, which, when dumped in a natural water system, causes environmental problems (Jabr et al. 2019; Krishnamoorthy et al. 2020, 2021). However, its collection, storage, transportation, and dosage are significant issues related to the direct use of urine in the fields. Hence, the recovery of nutrients in the form of struvite helps eliminate these bottlenecks and enhances the inherent properties necessary for a fertilizer (Siciliano 2016). Utilization of phosphate recovered from source-separated urine will reduce the impact on its non-renewable sources and help to close the nitrogen and phosphorus cycle. In addition to these environmental benefits, source-specific nutrient recovery will alleviate the cost associated with the overall process (Nageshwari and Balasubramanian 2022).

The production of struvite needs the input of adequate magnesium and other chemicals like alkali for pH to attain optimum conditions. Most wastewaters contain ammonium (NH_4^+) and phosphate (PO_4^{3-}) ions to induce struvite precipitation. Hence, the external supply of magnesium becomes necessary to attain the desired molar ratio (Tao et al. 2016). The most common method of struvite crystallization is by chemical precipitation, where Mg salts like MgO, $MgSO_4$, and $MgCl_2$ are added along with NaOH (García et al. 2013). The use of seawater and bittern as cheaper alternatives to Mg sources was also reported in previous studies (Crutchik and Garrido 2011). Though this method is easy and does not require any skilled labor, it has problems concerning decentralization and quality of struvite being produced.

In electrocoagulation, unlike chemical coagulation, the ions are supplied due to corrosion of the sacrificial anodes by applying an electric current. This process has been used in wastewater treatment technologies with high chemical oxygen demand (COD) (García et al. 2013) and complex structures such as landfill leachate (Tejera et al. 2021), textile wastewater (Bulca et al. 2021), slaughterhouse wastewater (Sandoval et al. 2022), automobile wastewater (Thakur 2021), etc., using different electrodes**.** This method offers several advantages like low treatment time, low cost, affordable, smooth operation, lower sludge production, reduction of secondary contamination, and flexibility to use for all types of wastewaters in a sustainable and eco-friendly approach. Other advantages include effective and rapid reduction of organic matter, minimum dependence on pH adjustment methods, and elimination of competitive anions (chlorine, sulphate, etc.) favoring maximum adsorptive removal of pollutants (Arab et al. 2022; Emamjomeh et al. 2020). In addition, it can also be used to remove heavy metals like arsenic, chromium, zinc and lead, oils, drugs, and pesticides from wastewaters by complexation, charge neutralization, entrapment, adsorption, or combination of these mechanisms (Akbay et al. 2019). The advanced electrocoagulation methods produce chemical oxidants such as hydroxyl radicals, which enhance pollutant removal by either increasing electrode dissolution or the oxidation reaction of the produced radical. The advanced methods of electrocoagulation are sono-electrocoagulation (sono-EC), photo-electrocoagulation (photo-EC), continuous-flow electrocoagulation, electromagnetic radiation-assisted treatment, peroxy-coagulation and peroxy-electrocoagulation, electrocoagulation, and membrane filtration. Though these methods are effective in pollutant removal; they are cost intensive (Garcia-Segura et al. 2017; Hashim et al. 2021; Abdulhadi et al. 2021).

Hug and Udert (2013) observed the feasibility of struvite precipitation using electrocoagulation in batch study using magnesium anode and stainless steel to recover 59–84% of phosphorus. They concluded that an anode potential of − 0.6 V vs. normal hydrogen electrode (NHE) suited the active release of magnesium producing struvite from source-separated stored urine. Song (2005) has reported the presence of an intermediate magnesium ion (Mg^+) species during the dissolution process. Upon further oxidation at the anode, it forms Mg^{2+} required for struvite formation. Meanwhile, the redox reaction at the cathode generates OH^- ion and hydrogen gas (Kékedy-Nagy et al. 2020).

The hydroxides produced by the cathode may lead to bubbles forming that produce turbulence in the solution, causing proper mixing of the compounds (Mores et al. 2016). The ionic conductivity of the solution affects the current, current efficiency, the voltage applied, and energy consumed by the system. Kruk et al. (2014) recovered PO_4^{3-} in the form of struvite from fermented waste-activated sludge and reported recovery of > 90% with pH 8.5 and current density 45.5 A m^{-2}. Many batch studies to evaluate the dependency of struvite on pH (Rajaniemi et al. 2021), current (Kruk et al. 2014) molar ratio, phosphorus, and nitrogen concentration (Kim et al. 2018) were done to obtain pure struvite using synthetic and real wastewater by electrocoagulation. A modification from previous studies using three coupled reactors (Huang et al. 2017), combination of struvite precipitation and ion exchange (Lin et al. 2018), and continuous reactor experiments (Wang et al. 2019; Rajaniemi et al. 2021) concluded the possibility of simultaneous nitrogen and phosphorus recovery but the its economic inefficiency was the major drawback for real-life application. A comparative analysis of recovery using pure magnesium and its alloy revealed 4.5 times greater efficiency of struvite precipitation is obtained when magnesium is free from any impurity. However, the pure magnesium is not much suitable for scale-up due to its proneness to passivation (Kékedy-Nagy et al. 2020).

The previous studies on electrocoagulation were carried out using iron and aluminum electrodes leading to the accumulation of these substances in the sludge, making their treatment process expensive, owing to the high energy consumed. However, magnesium is non-toxic and benefits plant growth when used with PO_4^{3-} and other nutrients. The comparison of various electrode materials to obtain the highest recovery is limited in the literature. In addition, the optimization studies were carried out using synthetic media, whose results cannot be mimicked due to the fluctuations caused by microbiota in wastewaters. Thus, nutrient recovery optimization using magnesium anode was needed to enhance its commercial applicability. The problem of pathogens and microorganisms in the urine poses a threat to safe urine fertilizers and studying ways to tackle this aspect for desired fertilizing application is lacking.

Furthermore, decentralization of struvite precipitation technology is difficult in the case of chemical precipitation techniques. To address these gaps in the literature and further promote scale-up, electrocoagulation of struvite was implemented, which is reliable, safe, and easy to operate. The present study optimizes the process influencing parameters for PO_4^{3-} recovery as struvite using magnesium (Mg) electrodes through electrocoagulation. One variable at a time (OVAT) approach was opted for optimizing the factors such as pH (6–9), electrode distance (0.5–3.5 cm), current (1.2–2 A), electrode material (Mg–carbon (C), Mg–aluminum (Al), Mg–stainless steel (SS), and Mg–Mg), and urine concentration (20–100%). In addition, the kinetics behind PO_4^{3-} recovery through electrocoagulation was elucidated. The effect of microbial population on phosphate recovery and yield was studied in various urine storage conditions such as fresh, stored, and autoclaved. Qualitative and quantitative analyses of the precipitate and left-over supernatant were performed using characterization tools such as Fourier transform infrared (FTIR) spectroscopy, X-ray diffraction (XRD), and scanning electron microscopy–energy dispersive X-ray spectrum (SEM-EDS). In a nutshell, the study focuses on integrated resource recovery, wastewater treatment, and production of struvite fertilizer to close the phosphorus loop.

Materials and methods

Urine collection and storage

Fresh human urine samples were collected in labeled collection bottles from healthy male individuals with a regular diet and between the age of 25–35. The samples collected were mixed and stored at − 20 °C. The urine samples with a pH less than 6.5 ± 0.3 were used as "fresh urine" for all the experiments, as a higher pH will indicate urea hydrolysis. The pH adjustment was made with 1M NaOH and 1M HCl prepared using deionized water. A portion of the sample was maintained at room temperature (25 ± 3 °C) for hydrolysis for use as "stored urine" as reported by Udert et al. (2003), as it takes at least 4 days for enzymatic hydrolysis of urea to ammonia and ammonium with simultaneous pH increase from 6 to 8 ± 0.3. The characteristics of fresh and stored urine are represented in Table 1. For autoclaved urine samples, a portion of the fresh urine was autoclaved under 15 psi saturated steam pressure at 121 °C for 15 min to eliminate the microbial population for use as a control in microbial study experiment.

Optimization experiments

The batch optimization experiments were performed using 1-L glass beakers (working volume: 800 mL) at room temperature (25 ± 3 °C) using a one variable at a time (OVAT) approach. The electrocoagulation set-up comprised a DC (direct current) power supply unit (multiple DC power MARS supply ME-230), magnetic stirrer (Tarson spinot digital), and a pair of anode and cathode connected to DC (Fig. 1). All the metal electrodes were procured from Sakthi Metals, Chennai (India), and carbon electrode from local suppliers. The electrodes were vertically and parallelly positioned in the reactor having an active surface area of 14 cm^2. They were completely immersed in the urine medium at a depth of 5 cm and ensured they did not touch the apparatus's bottom. The pH of the solution was initially maintained using 1 M NaOH and 1M HCl solutions. The increase in pH was attributed to the release of hydroxyl ions from the electrode as conducive to struvite formation. Based on literature survey, during the early experiments, interelectrode distance and current were fixed at 1.5 cm and 1.4 A, respectively, to optimize electrode material and pH. The reaction medium was agitated at 180 rpm using a hot-plate magnetic stirrer. Initially, the anode-cathode pair was varied (Mg–C, Mg–Al, Mg–SS, Mg–Mg) to assess the most suitable pair for efficienct PO_4^{3-} recovery. After each experiment, the anodes and cathodes were air dried.

Table 1 Characteristics of fresh and stored urine samples used for electrocoagulation of phosphate recovery as struvite

Characteristics	Fresh urine	Stored urine
pH	6.5 ± 0.3	8.0 ± 0.3
Conductivity (mS)	33.9 ± 0.5	53.9 ± 0.5
TDS (mg L^{-1})	7012.0 ± 410.0	11,475.0 ± 505.0
Salinity (mg L^{-1})	7.2 ± 0.5	12.8 ± 0.3
Sodium (mg L^{-1})	3800.0 ± 100.0	2100.0 ± 100.0
Potassium (mg L^{-1})	2310.0 ± 153.0	2000.0 ± 100.0
Calcium (mg L^{-1})	249.0 ± 32.0	36.0 ± 5.0
Phosphate (mg L^{-1})	1200.0 ± 55.0	849.0 ± 45.0

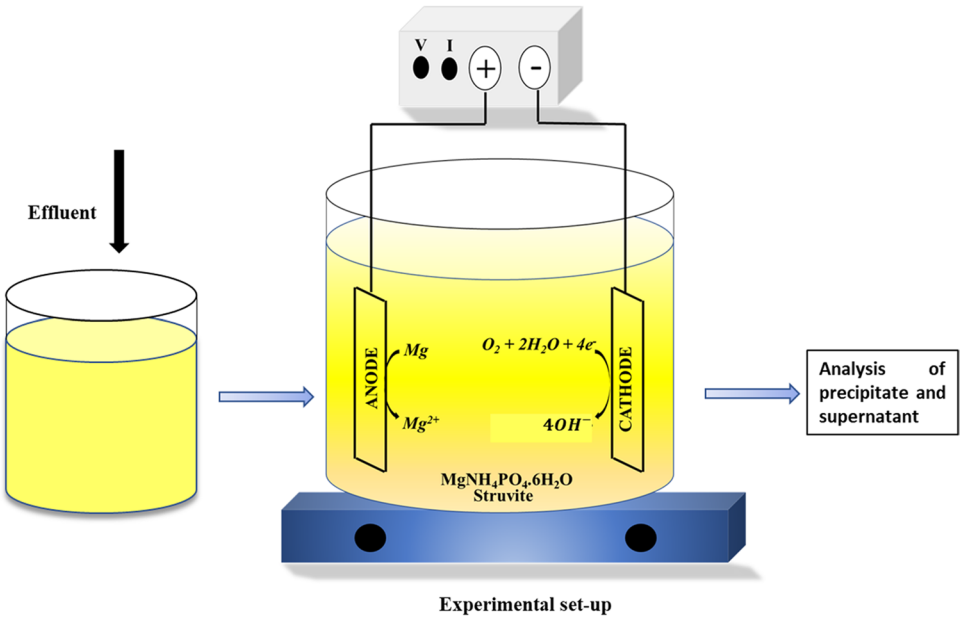

Fig. 1 Experimental set-up and mechanism of ion dissipation from electrodes for struvite recovery from human urine through electrocoagulation method

The precipitate formed on the surface was removed and cleaned using emery sheets and soaked in 1 M HCl solution followed by deionized water, making them suitable for further experiments. To estimate phosphate recovery and other parameters, a 10 mL urine sample was collected before and after the experiments and filtered using Whatman filter paper (0.4 µm pore size) before analysis. The phosphate recovery was calculated using Eq. (1) (Krishnamoorthy et al. 2020).

$$\text{Phosphate recovery} = \frac{P_0 - P_t}{P_0} \times 100 \tag{1}$$

where, P_0 and P_t are the initial and final phosphate concentrations (mg L^{-1}) before and after electrocoagulation, respectively.

pH optimization was carried out between 6 and 9, and the parameters optimized so far were fixed to further optimize interelectrode distance by altering 0.5–3.5 cm using an inert spacer to maintain the gap throughout the experiment. Current optimization experiments were done using current supply ranging between 1.2 and 2 A. This parameter can influence other dependent factors such as current efficiency, the molar ratio (Mg: P), energy consumption, and eventually PO_4^{3-} recovery (Eq. 1). Current efficiency and molar ratio were calculated by the formula given in Eqs. (2)–(5) (Kim et al. 2018).

$$\text{Current efficiency (\%)} = \frac{M_{\text{dissolved}}}{M_{\text{calculated}}} \times 100 \tag{2}$$

where $M_{\text{dissolved}}$ is the mass of magnesium dissolved (g) when a particular amount of current is applied (Eq. 3), and $M_{\text{calculated}}$ is the theoretical corrosion magnesium (g) calculated using Faraday's Law (Eq. 4).

$$M_{\text{dissolved}} = \left(P_0 - P_t\right) \times \frac{M_{\text{Mg}}}{M_{\text{P}}} + \left(m_t - m_o\right) \tag{3}$$

where P_o and P_t are initial and final PO_4^{3-} concentrations (mg L^{-1}); M_{Mg} is the molar mass of magnesium (24.3 g mol^{-1}); M_{P} is the molar mass of phosphorus (31 g mol^{-1}), and m_o and m_t are the concentrations of magnesium (mg L^{-1}) before and after electrocoagulation.

$$M_{\text{calculated}} = \frac{M_{\text{Mg}} \times I \times T}{n \times F \times v} \tag{4}$$

where $M_{\text{calculated}}$ is the theoretical mass of magnesium released, M_{Mg} is the molar mass of magnesium (23.4 g mol^{-1}), I is current in amperes, T is time in seconds, n is the valency of magnesium (2); F is Faraday's constant (96,485 C mol^{-1}), and v is the active volume (m^3).

$$\text{Molar ratio} = \frac{M_{\text{dissolved}}}{P_0} \times \frac{M_P}{M_{Mg}} \tag{5}$$

where $M_{\text{dissolved}}$ is the dissolved magnesium (Eq. 3), P_0 is the initial amount of PO_4^{3-} (mg L^{-1}) present in the sample, M_{P} is the molar mass of phosphorus (31 g mol^{-1}), and M_{Mg} is the molar mass (24.3 g mol^{-1}) of magnesium.

The reaction time was altered (30–60 min) to estimate the optimum period for maximum recovery and yield. The urine concentration was varied as 20, 40, 60, 80, and 100% by adding deionized water in respective ratios. After electrocoagulation, the precipitate yield was determined by measuring its dry weight. The experimental apparatus was kept

idle for 3 h to allow the precipitate to settle, and the residual supernatant was decanted and stored for further analysis. The precipitates settled at the bottom were centrifuged at 4000 rpm for 10 min and dried completely at 50 °C for 48 h in a hot air oven. All the experiments were carried out in triplicates, representing the standard deviation as error bars. The operational cost includes the electricity consumption, electrode material cost, and the cost of alkali chemicals. The formula used to calculate the price is given in Eqs. (6) and (7) (Akbay et al. 2019; Hashim et al. 2019).

$$\text{Operating Cost} = \alpha \times C_{\text{energy}} + \Upsilon \times C_{\text{electrode}} + \beta \times C_{\text{chemical}} \quad (6)$$

where α is the cost of electricity per kWh (Rs. 7 or 0.088 USD kWh^{-1} as per Govt. of Odisha, India tariff), Υ is the cost of magnesium electrode (3.3 USD kg^{-1}), and β is the unit cost of chemicals (NaOH = 8.06 USD)

$$C_{\text{energy}} = \frac{U \times I \times t}{1000 \times v \times \left(P_{0\_}P_t\right)} \quad (7)$$

where C_{energy} (kWh m^{-3}) is the electrical energy consumption, U is the voltage (V), I is the applied current (A), t is the electrolysis time (h), v is the active volume (m^3), and $(P_{0\_}P_t)$ is the phosphate recovered (mg L^{-1}). $C_{\text{electrode}}$ is calculated using Faraday's Law (Eq. 4), and C_{chemical} accounts for all the chemicals consumed during the reaction.

Microbial population study

To study the effect of microbial population on PO_4^{3-} recovery, urine samples were collected before and after electrocoagulation experiments. The samples were then serially diluted and plated on nutrient agar using the spread plate method. The petridishes were incubated at 37 °C overnight, and the colonies formed were numbered using the plate count technique, and the results were recorded as colony forming units (CFU per 100 mL).

Kinetic modeling

During electrocoagulation, the concentration of PO_4^{3-} decreases with the constant addition of magnesium ions over time. The various sets of reactions that occur at anode and cathode that lead to the formation of struvite and other precipitates are given in Eqs. (8)–(11) (Harrison et al. 2011; Song 2005)

$$\text{Anode}: \text{Mg} - e^- \rightarrow \text{Mg}^+ \quad (8)$$

$$\text{Mg}^+ + \text{H}_2\text{O} \rightarrow \text{Mg}^{2+} + \text{OH}^- + \frac{1}{2}\text{H}_2 \quad (9)$$

$$\text{Cathode}: \text{O}_2 + 2\text{H}_2\text{O} + 4e^- \rightarrow 4\text{OH}^- \quad (10)$$

$$\text{H}_2\text{O} + 2e^- \rightarrow \frac{1}{2}\text{H}_2 + 2\text{OH}^- \quad (11)$$

The Mg^{2+} ions dissipated at the anode combine with PO_4^{3-} and other ions in the solution lead to PO_4^{3-} recovery in the form of struvite and other phosphate salts as represented in Eqs. (12)–(14) (Kruk et al. 2014; Lin et al. 2018).

$$\text{Mg}^{2+} + \text{NH}_4^+ + \text{PO}_4^{3-} + 6\text{H}_2\text{O} \rightarrow \text{MgNH}_4\text{PO}_4.6\text{H}_2\text{O} \quad (12)$$

$$\text{Mg}^{2+} + \text{K}^+ + \text{PO}_4^{3-} + 6\text{H}_2\text{O} \rightarrow \text{MgKPO}_4.6\text{H}_2\text{O} \quad (13)$$

$$\text{Mg}^{2+} + \text{PO}_4^{3-} \rightarrow \text{Mg}_3\left(\text{PO}_4\right)_2 \quad (14)$$

To determine the mechanisms behind PO_4^{3-} recovery through electrocoagulation, various kinetic models such as first, second, pseudo-first order and pseudo-second order were studied. Under the optimized process conditions, samples were collected in 1-min intervals for the initial 16 min and increased to 3-min intervals for the remaining time. The equations of the intended kinetic models are given in Eqs. (15)–(18) (Bayuseno et al. 2020; Shahnaz et al. 2020).

$$\text{First order}: C_t = C_0 e^{-K_1 t} \quad (15)$$

where C_t (mg L^{-1}) is the concentration at electrolysis time t (min), K_1 (min^{-1}) is the rate constant of first-order kinetics, and C_0 is the initial concentration of PO_4^{3-} (mg L^{-1}).

$$\text{Second order}: \frac{t}{q} = \frac{1}{K_2} \times q_e^2 + \frac{t}{q_e} \quad (16)$$

where k_2 is the rate constant of the second-order adsorption, q_e is the adsorption capacity (mg g^{-1}), and t is the electrolysis time (min).

$$\text{Pseudo} - \text{first order}: \log\left(q_e - q_t\right) = \log q_e - \frac{k_1 t}{2.303} \quad (17)$$

$$\text{Pseudo} - \text{second order}: \frac{t}{q_t} = \frac{1}{k_2 q_e^2} + \frac{t}{q_e} \quad (18)$$

where K_1 (min^{-1}) and K_2 (mol L^{-1} s^{-1}) are the rate constants of pseudo-first order and pseudo-second order, respectively, q_t and q_e are the PO_4^{3-} recovered at a given time t and at equilibrium (mg g^{-1}), respectively. The correlation coefficient (R^2) was calculated to identify the most accurate kinetic model with the best fit.

Characterisation of the precipitates

The dried precipitate was analyzed by attenuated total reflectance-FTIR (MN344, Alpha ATR-FTIR, Bruker) to

assess the quality and functional group of the precipitate. XRD (Bruker, Germany) at a scan rate of 6° min^{-1} in the 2Θ range of 10–100 using cobalt lamp was carried out to identify the crystal characteristics. Further, the precipitates were subjected to SEM-EDS (JEOL JSM- 6480 LV, Oxford Instruments) to determine the morphology and elemental composition. The longitudinal size of the precipitates was determined by Image J software using SEM images.

Qualitative analysis of the residual supernatant urine

The physiochemical parameters of the residual supernatant after electrocoagulation, such as pH, conductivity, total dissolved solids (TDS), and salinity, were measured using a pH meter (Systronics digital pH meter 335) and multiparameter water quality meter (LMMP-30 Labman Scientific Instruments, India). The sodium and potassium concentrations were detected using a flame photometer (model 1385, ESICO, India). Calcium concentrations were evaluated using ion-selective electrodes (Vernier, USA). Magnesium concentration was estimated using the complexometric titration method using ethylenediamine tetraacetic acid (EDTA) and erichrome black T (EBT). Phosphate concentration was estimated using double beam UV–Vis spectrophotometer (model 2230, Systronics, India) using ammonium molybdate and stannous chloride at the absorbance of 650 nm.

Results and discussion

Optimization of process affecting parameters

Electrode material

Different anode-cathode pairs were studied to evaluate the optimum electrodes required for the maximum recovery of phosphate. The anode material was fixed to be Mg to facilitate ion dissipation for struvite crystallization, and the cathodes were of carbon, stainless steel, aluminum, and magnesium. The results of phosphate recovered and yield using each pair of electrodes are shown in Fig. 2a. The removal efficiencies are 57.15, 87.3, 88.65, and 93.55% for Mg–Al, Mg–C, Mg–SS, and Mg–Mg electrodes, respectively. The Mg–Mg pair provided the highest recovery, possibly because of the spontaneous release of Mg from the electrode even in the absence of electricity. Due to low standard reduction potential of Mg ($E^{\circ}_{Mg^{2+}/Mg} = -2.372\ V\ vs.SHE$) (Coates 1945) and its alloys, Mg dissolves in aqueous solution producing Mg^{2+} ions and H_2 bubbles (Kékedy-Nagy et al. 2020). A simultaneous porous oxide layer of MgO on the inner side and $Mg(OH)_2$ on the outer side is formed with time, making the magnesium anode polarized (Cai et al. 2022). This phenomenon of negative difference effect (NDE) was observed in Mg electrodes. The cathodic and anodic reactions simultaneously increase on the current application, further accelerating the hydrogen evolution reaction.

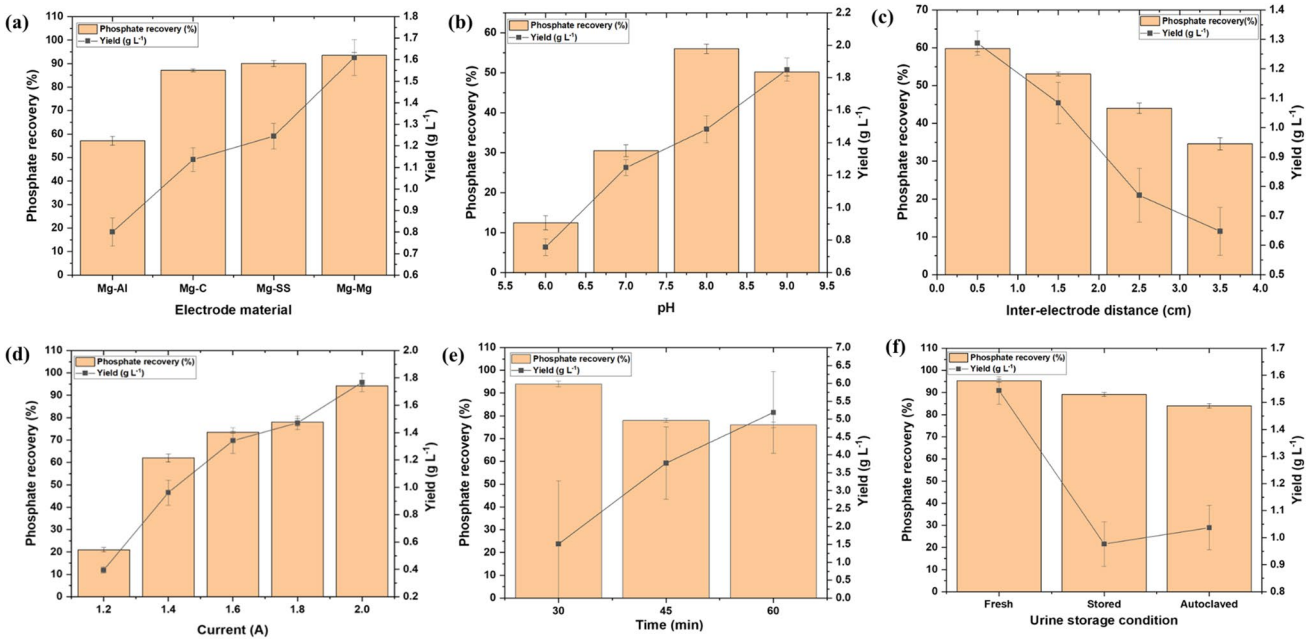

Fig. 2 Effect of influencing parameters **a** electrode material (Mg–Al, Mg–C, Mg–SS, Mg–Mg); **b** pH (6–9); **c** interelectrode distance (0.5–3.5 cm); **d** current (1.2–2.0 A); **e** reaction time (30–60 min); and **f** urine concentration (20–100%) on phosphate recovery as struvite

In the case of the Mg sacrificial anode, the corrosion occurs in four different ways: self-corrosion, loss of metal in the form of chunks, formation of monovalent ions, and charge waste due to hydrogen evolution (Kruk et al. 2014). These possible explanations justify efficient ion release when Mg is used as anode and cathode for better PO_4^{3-} recovery. On the contrary, in other electrodes like iron, zinc, and steel, the increase in anodic reactions decreases the cathodic reactions (Kim et al. 2018). Higher galvanic corrosion occurs when Mg is paired with SS compared to other materials due to the deposition of Fe^{2+} as an impurity on the Mg anode. This activity decreases its polarization resistance, making it more reactive. On the other hand, Al^{3+} corrosion during the reaction promotes the formation of passivating layer ($Al(OH)_3$, Al_2O_3) on the Mg anode (Bagastyo et al. 2022). Hence, the Mg–Mg electrode pair was used for the remaining set of experiments.

pH

The conductivity of the solution is affected by the change in pH which further affects various factors of the electrocoagulation system influencing the phosphate recovery efficiency; hence, optimizing pH becomes important (Naje et al. 2016). In the current study, the recovery of PO_4^{3-} was 12.5% when the initial urine pH was 6. An increase in pH from 6 to 7 doubled the recovery of PO_4^{3-} to 30.5%. Many studies have concluded the occurrence of struvite below the pH of 7 (Doyle and Parsons 2002; Zeng and Li 2006). However, with the further increase, the recovery reached 56%, after which the trend formed a plateau. An increase in pH in the solution increases the ammonium ion, which contributes to struvite precipitation and increases the yield (Chipako and Randall 2020). The optimum pH for struvite precipitation was reported to be between 8.5 and 9.4 (García et al. 2013). In an electrocoagulation system, due to continuous production of OH^- through oxygen reduction and hydrogen production, pH and saturation index increase with time, leading to a decrease in precipitate solubility (Kruk et al. 2014). However, a decrease in recovery with pH shift from 8 to 9 was observed, which could be because of the increase in solubility of PO_4^{3-} salts with pH (Fig. 2b) (García et al. 2013). An increase of pH above 10 favors brucite formation, limiting the ions available for struvite recovery and accelerating passivation (Bagastyo et al. 2022). Hence, the precipitate yield increased with pH, which could be due to the formation and deposition of insoluble $Mg(OH)_2$ and other Mg salts along with the precipitate (Pilarska et al. 2017; Lin et al. 2018). Hence, the optimum pH for the highest phosphate recovery was concluded as 8.

Interelectrode distance

The interelectrode distance (IED) plays a significant role in the electrocoagulation system due to its direct association with the electrostatic field. The effect of IED on precipitation was investigated with Mg–Mg electrodes at pH 8 by varying the IED from 0.5 to 3.5 cm. The results of the experiments are shown in Fig. 2c, where a decrease in phosphorus recovery and yield with an increase in IED can be noticed. The increased distance between the electrodes could have decreased the electrostatic effect, slowing down the formation of ions (Naje et al. 2016). Higher electrode distance increases the time of ion transfer due to an increase in resistance, which in turn decreases the current intensity and, ultimately, the formation of Mg^{2+} ions and PO_4^{3-} recovery (Moradi et al. 2021). It can be observed that the recovery of phosphate increased from 53.5 to 59.8% when IED was decreased from 1.5 to 0.5 cm. This shows that less electrode gap is desirable as a higher IED increases the resistance between electrodes, delaying the corrosion of the anode and, in turn, decreasing the precipitate yield (Mohora et al. 2012; Hug and Udert 2013). Similar results have been reported by Rajaniemi et al. (2021) for struvite precipitation from synthetic and humic acid wastewater with Mg–Mg electrode distance of 0.5 cm and achieved 93.6% PO_4^{3-} recovery.

Current

Recovery of phosphate under the influence of various amperages was performed by maintaining the pH (8) and IED (0.5 cm) constant. With the current increase from 1.2 to 1.4 A, phosphate recovery showed a threefold increase from 21 to 62%, which corresponds to the higher release of Mg ions with the increment in current. When the current is low, the power of the electrode to form ions (coagulant) becomes less, decreasing the removal of phosphate (Asgharian et al. 2017). With the current increase, the production of Mg^{2+} and OH^- ions in the solution increases, affecting the pH and the molar ratio, thereby influencing PO_4^{3-} recovery (Huang et al. 2017). According to Faraday's law, Mg released from the anode is directly proportional to the current applied as shown in Eq. (4). The phosphate recovery increased up to 94% when the current applied was 2 A. With the increase of current, high Mg release could have occurred that resulted in high Mg:P and current efficiency. Current efficiency of less than 100% indicates the occurrence of corrosion without applying current (Kruk et al. 2014). In this study, current efficiency for all the experiments was above 200% and kept on increasing with the increase in current supply. Overall, higher current at lower duration is beneficial for PO_4^{3-} recovery. Table 2 shows the effect on varying current on other factors such as current efficiency, Mg:P ratio, and energy consumption. Zhou and Chen (2019) also reported an increase in the precipitate yield and purity with an increase in current. However, further increased current does not significantly impact the PO_4^{3-} recovery due to the formation of a passivation layer on the anode surface that

reduces the dissolution of Mg into the solution. The phenomenon of passivation is also reported in other studies by Hug and Udert (2013). These results can be corroborated with the PO_4^{3-} and yield values obtained in this study with an increase in current (Fig. 2d).

Reaction time

The recovery was 94% with the electrolysis time of 30 min and decreased to 78 and 56%, with the increment of time from 45 to 60 min, respectively (Fig. 2e). The increase of reaction time rises the pH of the solution; thus, a higher yield was reported with the reduction of phosphate recovery (Li et al. 2020). Such observations can be justified by considering the increase of solubility of phosphate salts at high pH, the unavailability of the ammonium ion for struvite precipitation due to its conversion to volatile ammonia, and the increase of bonding between Mg^{2+} and OH^- than the phosphate ions (Siciliano et al. 2020; Krishnamoorthy et al. 2020).

Urine concentration

The effect of different urine concentrations (20, 40, 60, 80, and 100%) was estimated using parameters optimized from the previous experiments. The results as observed in Fig. 2f show an increase in phosphate recovery as the dilution of the solution decreases. The conductivity of the solution is an important factor for the transfer of current between solutes and the applied voltage. With the increase of dilution, the conductivity of the solution decreases, resulting in more energy required to overcome the resistance between anode and cathode, thereby decreasing the PO_4^{3-} recovery (Moradi et al. 2021). Initially, PO_4^{3-} recovery increases when Mg is supplied from anode, but with time the amount of phosphate becomes limiting, reducing the recovery. The lower rate of removal due to decrease of PO_4^{3-} in the solution may be attributed to higher N:P ratio (Kruk et al. 2014). However, the difference in PO_4^{3-} recovery with urine dilution is very low. Passing high current in low PO_4^{3-} concentration solution attributes to rapid increase of pH in the solution favoring the production of $Mg(OH)_2$ (Bagastyo et al. 2022). Hence, the presence of $Mg(OH)_2$ may be the probable reason for the increase in precipitate yield when magnesium ions are excess in the solution compared to PO_4^{3-} for attaining the stoichiometric value required for precipitation of struvite. $Mg(OH)_2$ is also insoluble in water and hence does not contribute to the increase in solution pH (Doyle and Parsons 2002; García et al. 2013).

Table 2 Effect of current on phosphate recovery as struvite and its energy consumption

Current (A)	Current efficiency (%)	Mg: P	Energy consumption (kWh m^{-3})	Recovery rate (%)
1.2	146	0.35	0.080	21
1.4	225	0.75	0.035	62
1.6	236	0.88	0.036	74
1.8	243	1.02	0.038	80
2	251	1.20	0.032	94

Effect of the microbial community in various urine storage conditions on phosphate recovery

The effect of the microbial community in the urine on the PO_4^{3-} recovery and yield was evaluated using fresh, stored, and autoclaved urine. The electrocoagulation experiment performed on urine storage conditions showed less difference in the PO_4^{3-} recovery process. The recovery was high in fresh urine by about 95%, followed by stored and autoclaved urine, having 89.15% and 84% recoveries, respectively (Fig. 3a). However, the yield of autoclaved urine is slightly higher than stored urine as 90% of the total nitrogen gets converted to ammonia during storage, which is volatile and only 1% of nitrogen remains available in the form of ammonium ion for precipitation (Udert et al. 2006). The phosphorus amount is less due to spontaneous precipitation of struvite and calcium phosphate, which can be a reasonable explanation for less yield in stored urine (Hug and Udert 2013).

After the electrocoagulation experiments, the reduction of the microbial population was around 98–99% in both the fresh and stored urine storage conditions (Fig. 3b). The microbial population was observed to be high in stored urine before the electrocoagulation experiment as compared to fresh urine The urine of a healthy individual with normal diet contains around 181–611 OTU (operational taxonomical unit) dominated by few taxa. Stored urine has more quantity of microbes, but the diversity is less due to the inhibition by high concentration of ammonia produced during the hydrolysis process (Lahr et al. 2016). The decrease of the microbial population might be the physical elimination or chemical deactivation of pathways by getting entrapped in the flocs, destabilization, or demobilization of the cell envelope by the electric field or reactive oxygen species (Ghernaout et al. 2019). Many studies have concluded that the electrocoagulation process eliminates bacteria from river water, surface water, synthetic water, and industrial wastewater (Chellam and Sari 2016).

Determination of phosphate recovery kinetics

To determine the order of reaction kinetics of PO_4^{3-} recovery, experiments were carried out to monitor the variation

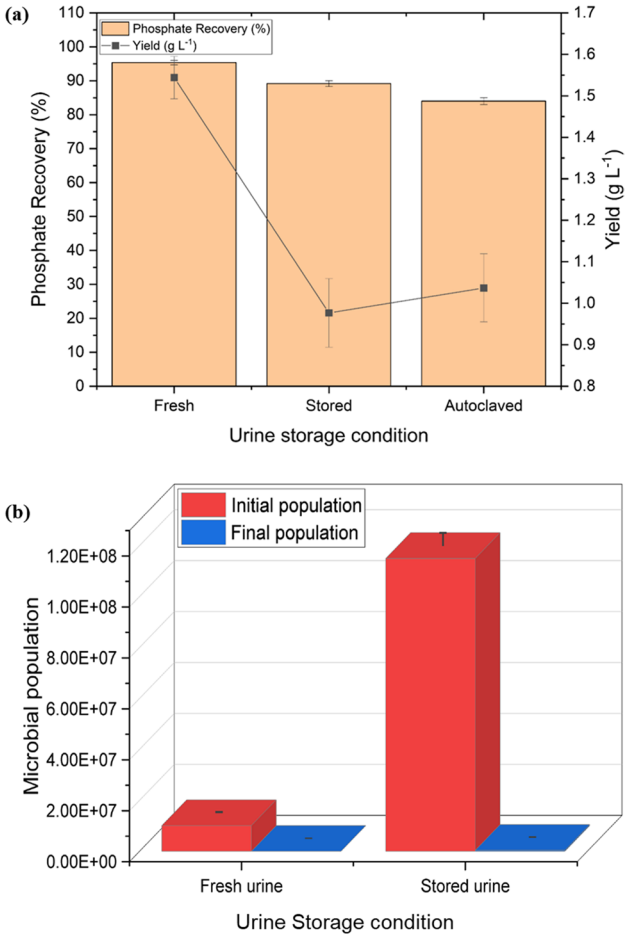

Fig. 3 **a** Effect of urine storage conditions (fresh, stored, and autoclaved) on phosphate recovery and struvite yield; **b** effect of electrocoagulation on microbial population of different urine storage conditions (fresh, stored)

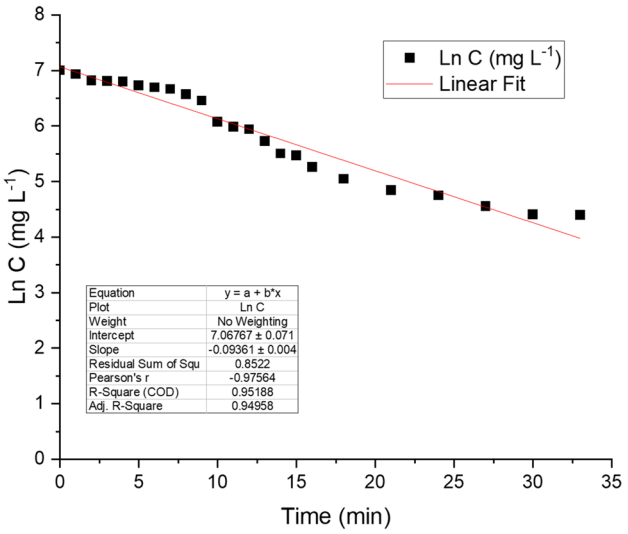

Fig. 4 First-order kinetic curve of electrocoagulation method of phosphate recovery as struvite using the optimised conditions (pH 8, 0.5-cm IED, 2 A, 100% urine, Mg–Mg electrodes, and 30 min reaction time) of the study

in PO_4^{3-} concentration with time during recovery through electrocoagulation. The data obtained were fitted in different kinetic models (first order, second order, pseudo-first order and pseudo-second order) to assess the best fit. The results concluded that the recovery of PO_4^{3-} through electrocoagulation follows first-order kinetics with a correlation coefficient (R^2) value of 0.9518, as shown in Fig. 4. The slope value (k) lies between 0.08 and 0.09, corresponding to the rate constant between 5.34 to 5.89 h^{-1}. Luo et al. (2022) reported phosphorus recovery from chicken slurry manure followed first-order reaction using magnesium anode to produce pure struvite. Tibebe et al. (2019) also confirmed that the PO_4^{3-} recovery by electrocoagulation is a first-order reaction. The study was conducted using an aluminum electrode from synthetic wastewater. Recovery depends on the initial concentration of PO_4^{3-} where the recovery was initially higher due to more availability of PO_4^{3-}, but gradually the removal rate slows down when PO_4^{3-} becomes limiting.

Similar results were also reported by Zhang et al. (2016) for 96.7% PO_4^{3-} recovery from animal manure using low carbon steel, where the reaction kinetics was found to be of the first order.

Qualitative analysis of the precipitate

The precipitates were characterized using sophisticated techniques such as FTIR, XRD, and SEM-EDS. According to the peaks identified in Fig. 5, the absorption peaks occurring at 3774, 3658, 3616, and 3556 cm^{-1} are due to O–H and N–H stretching. The N–H bending corresponding to NH_4^+ group is present at 1426 and 1457 cm^{-1}. The intensities of bands between 1685 and 1514 cm^{-1} are OH bending in precipitate obtained from fresh urine. The stored urine precipitate has OH bending bands in 1524, 1661, and 1697 cm^{-1}. The band's intensity at 983 cm^{-1} represents the bending vibrations of PO_4, and peaks at 744 and 683 cm^{-1} indicate metal oxygen bending, which in this case was found to be Mg–O. The FTIR spectrum proves the existence of PO_4^{3-}, NH_4^+, O–H, and metal-oxygen bands, making the spectra identical to that of struvite as confirmed in previous studies (Frost et al. 2005; Kurtulus and Tas 2011; Suguna et al. 2012; Yetilmezsoy et al. 2017). The transmission of PO_4 is higher in fresh urine samples than in stored ones. This could be because of the high concentration of PO_4^{3-} in fresh urine, which gets lost upon storage due to spontaneous precipitation of phosphate salts (Krishnamoorthy et al. 2020).

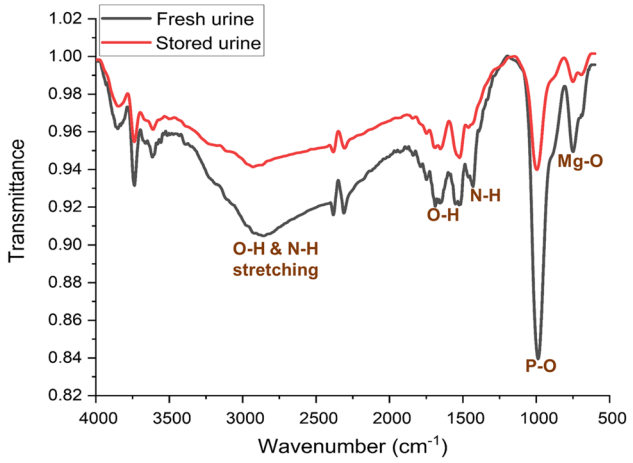

Fig. 5 Fourier transform infrared spectrum of the precipitate from fresh urine and stored urine samples produced at optimized conditions of pH 8, 0.5 cm IED, 2 A, 100% urine, Mg–Mg electrodes, and 30 min reaction time

The XRD analysis indicated the precipitation of struvite (Fig. 6a and b) in both the storage conditions. The peaks of electrochemically produced struvite were found to be close to the standard struvite crystal peak pattern (ICDC # 077-2303). The difference in the intensity of the peaks in fresh and stored urine samples might indicate the difference of structure (Kékedy-Nagy et al. 2019). There were no additional peaks observed that would correspond to the presence of any impurities (Kruk et al. 2014). Thus, the produced struvite can be considered pure.

SEM analysis revealed the morphology of crystals precipitated from fresh urine to be rod shaped. In the case of stored urine precipitate, the crystals are compact and aggregated due to a low concentration of PO_4^{3-} and high supersaturation value, leading to more crystal formation and spontaneous agglomeration (Andreev et al. 2017). However, Chauhan and Joshi (2014) reported the presence of various morphology of crystals such as needle, feather, and prismatic, which were still confirmed to be struvite. EDS

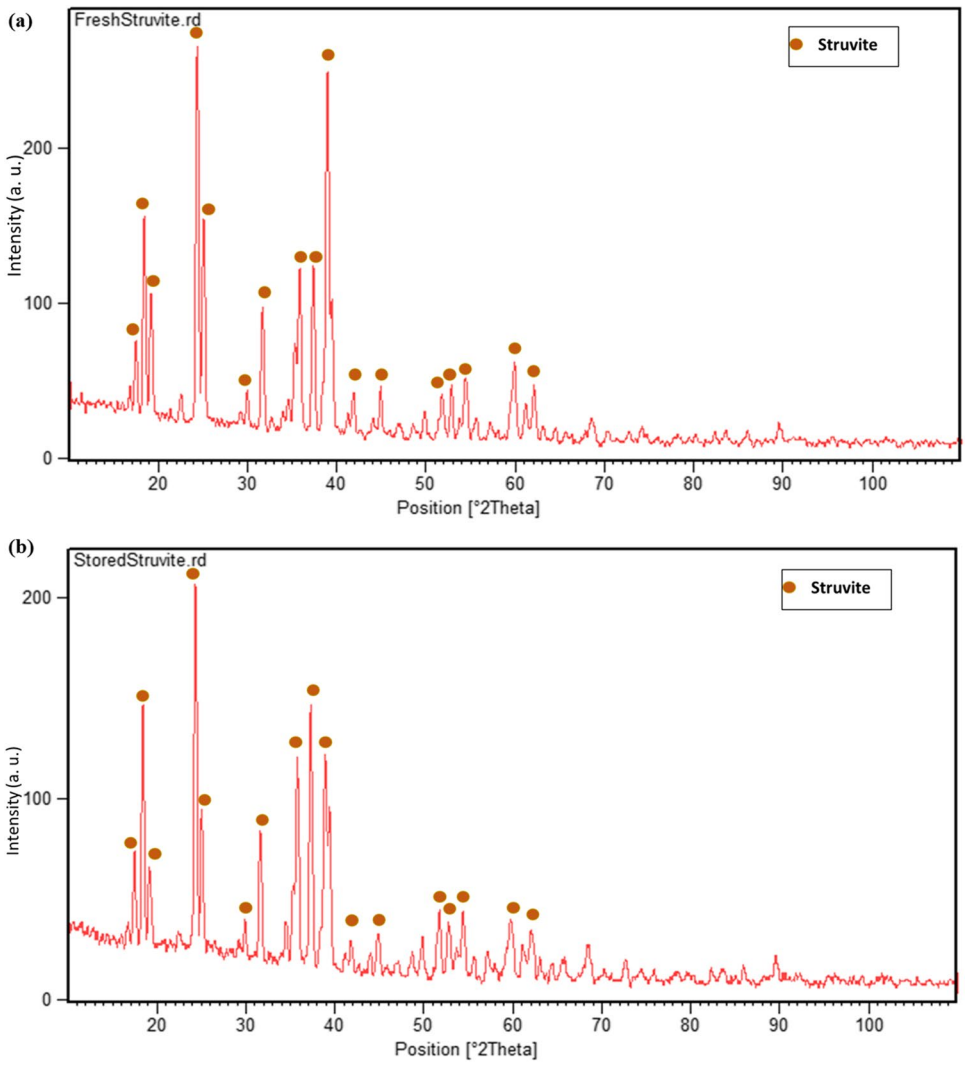

Fig. 6 X-ray diffraction spectra for the precipitate from **a** fresh urine and **b** stored urine samples produced at optimized conditions of pH 8, 0.5-cm IED, 2 A, 100% urine, Mg–Mg electrodes, and 30 min reaction time

data confirmed high content of Mg, P, and O (Fig. 7a and b), which are the main elements of struvite (Heraldy et al. 2017). The crystal sizes in both the samples are smaller ranging from 0.5 to 2.5 µm in stored urine and 4 to 12 µm in fresh urine as shown in Fig. 8. The nutrient content of P in fresh and stored urine struvite was found to be 31.10 and 35.12%, respectively, further supporting the FTIR results.

Effect of electrocoagulation on the residual supernatant quality

After PO_4^{3-} recovery through electrocoagulation, the residual supernatant was collected and characterized for physicochemical parameters and residual phosphate. The pH of the solution increased from 8 to 10 due to the release of OH^- as shown in Eqs. (8)–(11). The conductivity, TDS, and salinity were reduced by 41.6, 42.9, and 45.5%, respectively, for all the urine sample left-over after the struvite-recovery experiments. Reductions in the concentration of ions like sodium (50.8%), potassium (49.7%), and calcium (30.5%), apart from phosphate and ammonium, were also observed. Similar results were recorded by Jose et al. (2019) where an 86% TDS reduction was detected along with conductivity, COD, TOC, and color when the residual liquid after chemical retting of coconut fiber was treated with electrocoagulation using six electrodes at a current of 100 mA for 90 min. Heffron et al. (2016) also reported the reduction of ions by the electrocoagulation process.

Energy and operational cost

For PO_4^{3-} recovery from undiluted urine using Mg–Mg electrodes under the optimized conditions, the operating cost was calculated using Eqs. (6)–(8). The electrode material consumption, energy consumption, and chemical cost were determined to be 0.121 kg m^{-3}, 0.0724 kWh m^{-3}, and 0.003 kg m^{-3}, respectively. The overall cost for struvite production was calculated to be 0.194 USD m^{-3}. Previous studies for electrolytic struvite precipitation have compared only the cost of magnesium sources, reporting Mg anode feasible in terms of cost and purity of the crystals (Hug and Udert 2013; Lin et al. 2018). Wang et al. (2019) have reported the cost of struvite production from 50-L electrolyzer containing swine wastewater to be 0.21 USD kg^{-1}. The cost of treating authentic wastewater and struvite production was found to be 0.94 USD m^{-3} in batch electrocoagulation method by Rajaniemi et al. (2021). The cost of 0.94 USD m^{-3} was reported for PO_4^{3-} removal by electrocoagulation using iron rods by Akbay et al. (2019). Hashim et al. (2019) observed 99% phosphate removal by treating river water for 60 min using an aluminum electrode with the operating cost of 0.503 USD m^{-3}. Omwene and Kobya (2018) detected 99% phosphate removal by electrocoagulation at pH 4 using aluminum for 60 min and iron for 100 min incurring costs of 1.032 and 1.343 USD m^{-3}, respectively. Tejera et al. (2021) have observed reduction of overall cost from 5.91 to 3.48 USD kg^{-1} of wastewater for COD removal using the

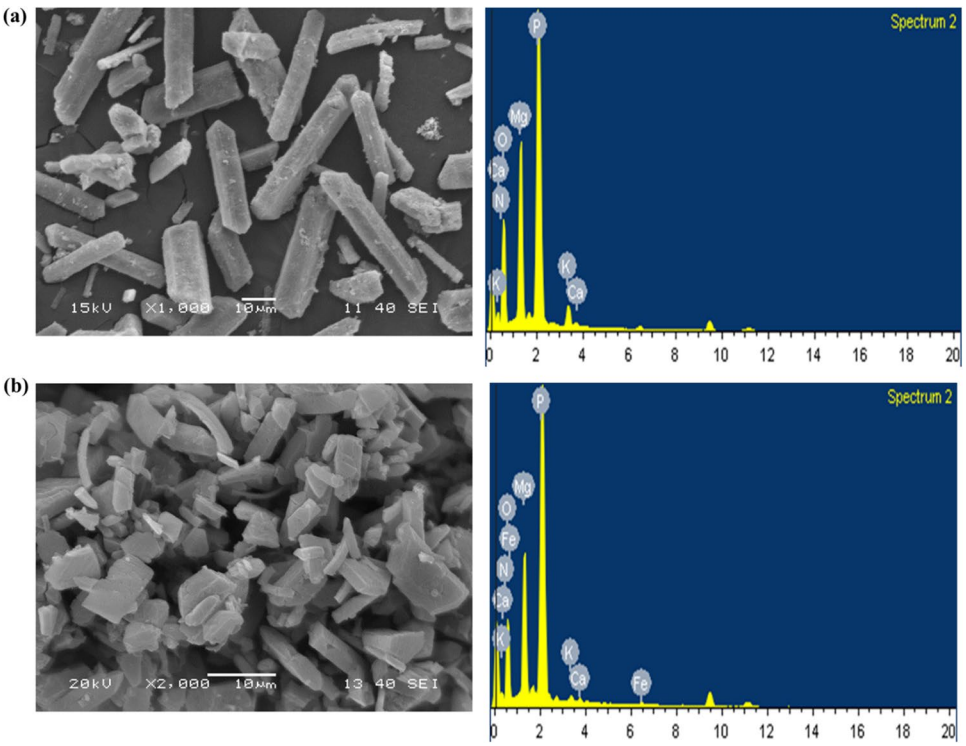

Fig. 7 Scanning electron microscopic images of recovered precipitate from **a** fresh urine and **b** stored urine samples produced at optimized conditions (pH 8, 0.5-cm IED, 2 A, 100% urine, Mg–Mg electrodes, and 30-min reaction time) along with its elemental composition obtained through energy X-ray dispersive spectroscopy

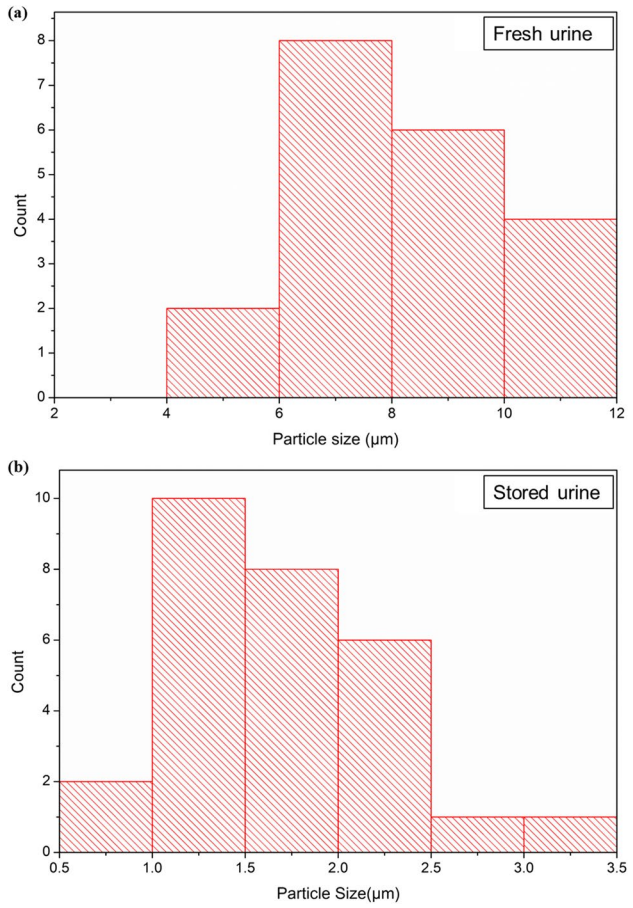

Fig. 8 Crystal size of struvite precipitates obtained from **a** stored urine and **b** fresh urine produced under optimized conditions of pH 8, 0.5-cm IED, 2 A, 100% urine, Mg–Mg electrodes, and 30-min reaction time

combination of electrocoagulation and Fenton process. It can be observed that the overall cost of production is quite low as compared to other studies of PO_4^{3-} removal using electrocoagulation. This could be due to the low cost of magnesium electrodes and their sacrificial anode property, which helps in better dissociation of ions (macro-corrosion) quickly. As discussed earlier, magnesium's reduction potential is lower than other metals used in earlier studies, making them more suitable for phosphate recovery by electrocoagulation (Hug and Udert 2013).

Conclusion

Characterization results revealed that phosphate (PO_4^{3-}) recovery through electrocoagulation occurs in the formation of struvite crystals. Optimization of influential process conditions (pH 8, 0.5-cm interelectrode distance, 2 A current, and electrolysis time of 30 min using Mg–Mg electrodes in undiluted urine medium) resulted in a maximum struvite recovery of 95%. Based on the PO_4^{3-} recovery, nutrient composition of struvite and its quality, fresh urine was found to serve as a better source for struvite precipitation. The kinetic studies confirmed that PO_4^{3-} recovery through electrocoagulation follows the first order. Analysis of residual supernatant showed a reduction in TDS, conductivity, salinity, and other ions like Na^+, K^+, and Ca^{2+}. In addition, the microbial population decreased by 99%, making them suitable for irrigation upon minimal post-treatment, which can further reduce the water footprint. However, anode passivation, foaming, and release of foul odor occurring during the process can reduce the efficiency of the process and generate problems in large-scale operations. These limitations have to be addressed in future studies to make struvite production through electrocoagulation more reliable and scalable.

Acknowledgements The authors thank the Department of Biotechnology and Medical Engineering of National Institute of Technology Rourkela for providing the necessary research facilities. The authors greatly acknowledge the Department of Science and Technology (DST), Government of India (GoI), for sponsoring the research.

Author contribution The study conceptual design was made by Alisha Zaffar and Balasubramanian Paramasivan. Experiments, data collection and analysis were performed by Alisha Zaffar and Nahaarjun Nagaraj. Alisha Zaffar and Nageshwari Krishnamoorthy performed the characterisation and drafted the manuscript. Sivaraman Jeyaraman and Balasubramanian Paramasivan have reviewed and edited the manuscript. All authors have read and approved the final manuscript.

Funding This research work was financially sponsored by Department of Science and Technology (DST), Government of India (GoI) under Agro-Technology Development Programme [File No. DST/TDT/Agro43/2020].

Data availability The dataset used during the current research are available from the corresponding author on reasonable request.

Declarations

Ethical approval Not applicable.

Consent to participate Not applicable.

Consent for publication All authors allow the publication of the paper.

Competing interests The authors declare no competing interests.

References

Abdulhadi B, Kot P, Hashim K, Shaw A, Muradov M, Al-Khaddar R (2021) Continuous-flow electrocoagulation (EC) process for iron removal from water: experimental, statistical and economic study. Sci Total Environ 760:143417. https://doi.org/10.1016/j.scitotenv.2020.143417

Asgharian F, Khosravi-Nikou MR, Anvaripour B, Danaee I (2017) Electrocoagulation and ultrasonic removal of humic acid from wastewater. Environ Prog Sustain Energy 36(3):822–829. https://doi.org/10.1002/ep.12512

Andreev N, Ronteltap M, Boincean B, Wernli M, Zubcov E, Bagrin N, Borodin N, Lens PNL (2017) Lactic acid fermentation of human urine to improve its fertilizing value and reduce odour emissions. J Environ Manag 198:63–69. https://doi.org/10.1016/j.jenvman.2017.04.059

Arab M, Faramarz MG, Hashim K (2022) Applications of computational and statistical models for optimizing the electrochemical removal of cephalexin antibiotic from water. Water 14(3):344

Bagastyo AY, Anggrainy AD, Khoiruddin K, Ursada R, Warmadewanthi IDAA, Wenten IG (2022) Electrochemically-driven struvite recovery: prospect and challenges for the application of magnesium sacrificial anode. Sep Purif Technol 120653. https://doi.org/10.1016/j.seppur.2022.120653

Bayuseno AP, Perwitasari DS, Muryanto S, Tauviqirrahman M, Jamari J (2020) Kinetics and morphological characteristics of struvite ($MgNH_4PO_4.6H_2O$) under the influence of maleic acid. Heliyon 6(3):03533. https://doi.org/10.1016/j.heliyon.2020.e03533

Bulca Ö, Palas B, Atalay S, Ersöz G (2021) Performance investigation of the hybrid methods of adsorption or catalytic wet air oxidation subsequent to electrocoagulation in treatment of real textile wastewater and kinetic modelling. J Water Process Eng 40:101821. https://doi.org/10.1016/j.jwpe.2020.101821

Cai Y, Han Z, Lin X, Du J, Lei Z, Ye Z, Zhu J (2022) Mechanisms of releasing magnesium ions from a magnesium anode in an electrolysis reactor with struvite precipitation. J Environ Chem Eng 10(1):106661. https://doi.org/10.1016/j.jece.2021.106661

Chauhan CK, Joshi MJ (2014) Growth and characterization of struvite-Na crystals. J Cryst Growth 401:221–226. https://doi.org/10.1016/j.jcrysgro.2014.01.052

Chellam S, Sari MA (2016) Aluminum electrocoagulation as pretreatment during microfiltration of surface water containing NOM: a review of fouling, NOM, DBP, and virus control. J Hazard Mater 304:490–500. https://doi.org/10.1016/j.jhazmat.2015.10.054

Chipako TL, Randall DG (2020) Urine treatment technologies and the importance of pH. J Environ Chem Eng 8(1):103622. https://doi.org/10.1016/j.jece.2019.103622

Crutchik D, Garrido JM (2011) Struvite crystallization versus amorphous magnesium and calcium phosphate precipitation during the treatment of a saline industrial wastewater. Water Sci Technol 64:2460–2467. https://doi.org/10.2166/wst.2011.836

Doyle JD, Parsons SA (2002) Struvite formation, control and recovery. Water Res 36(16):3925–3940. https://doi.org/10.1016/S0043-1354(02)00126-4

Coates GE (1945) The standard electrode potential of magnesium. J Chem Soc (Resumed) 124:478–479

Emamjomeh M, Kakavand S, Jamali H, Alizadeh SM, Safdari M, Mousavi SE, Hashim KS, Mousazadeh M (2020) The treatment of printing and packaging wastewater by electrocoagulation–flotation: the simultaneous efficacy of critical parameters and economics. Desalin Water Treat 205. https://doi.org/10.5004/dwt.2020.26339

Frost RL, Weier ML, Martens WN, Henry DA, Mills SJ (2005) Raman spectroscopy of newberyite, hannayite and struvite. Spectrochimica Acta – Part A: Molecular and Biomolecular Spectroscopy 62:181–188. https://doi.org/10.1016/j.saa.2004.12.024

García FP, Hernández JC, Cruz VER, Santillan YM, Marzo MAM, Avila JH, Moreno FP (2013) Recovery and characterization of struvite from sediment and sludge resulting from the process of acid whey electrocoagulation. Asian J Chem 25:8005–8009. https://doi.org/10.14233/ajchem.2013.14933

Garcia-Segura S, Eiband MMS, de Melo JV, Martínez-Huitle CA (2017) Electrocoagulation and advanced electrocoagulation processes: A general review about the fundamentals, emerging applications and its association with other technologies. J Electroanal Chem 801:267–299. https://doi.org/10.1016/j.jelechem.2017.07.047

Ghernaout D, Touahmia M, Aichouni M (2019) Disinfecting water: electrocoagulation as an efficient process. Applied. Engineering 3:1–12. https://doi.org/10.11648/j.ae.20190301.11

Harrison ML, Johns MR, White ET, Mehta CM (2011) Growth rate kinetics for struvite crystallisation. Chem Eng Trans 25:309–314

Hashim KS, Al Khaddar R, Jasim N, Shaw A, Phipps D, Kot P, Pedrola MO, Alattabi AW, Abdulredha M, Alawsh R (2019) Electrocoagulation as a green technology for phosphate removal from River water. Sep Purif Technol 210:135–144. https://doi.org/10.1016/j.seppur.2018.07.056

Hashim KS, Shaw A, AlKhaddar R, Kot P, Al-Shamma'a A (2021) Water purification from metal ions in the presence of organic matter using electromagnetic radiation-assisted treatment. J Clean Prod 280:124427. https://doi.org/10.1016/j.jclepro.2020.124427

Heffron J, Marhefke M, Mayer BK (2016) Removal of trace metal contaminants from potable water by electrocoagulation. Sci Rep 6:1–9. https://doi.org/10.1038/srep28478

Heraldy E, Rahmawati F, Heriyanto PDP (2017) Preparation of struvite from desalination waste. J Environ Chem Eng 5:1666–1675. https://doi.org/10.1016/j.jece.2017.03.005

Huang H, Zhang D, Li J, Guo G, Tang S (2017) Phosphate recovery from swine wastewater using plant ash in chemical crystallization. J Clean Prod 168:338–345. https://doi.org/10.1016/j.jclepro.2017.09.042

Huang H, Liu J, Xiao J, Zhang P, Gao F (2016) Highly efficient recovery of ammonium nitrogen from coking wastewater by coupling struvite precipitation and microwave radiation technology. ACS Sustain Chem Eng 4:3688–3696. https://doi.org/10.1021/acssuschemeng.6b00247

Hug A, Udert KM (2013) Struvite precipitation from urine with electrochemical magnesium dosage. Water Res 47:289–299. https://doi.org/10.1016/j.watres.2012.09.036

Jabr G, Saidan M, Al-Hmoud N (2019) Phosphorus recovery by struvite formation from Al Samra municipal wastewater treatment plant in Jordan. Desalin Water Treat 146:315–325. https://doi.org/10.5004/dwt.2019.23608

Jaafari J, Javidb AB, Barzanounic H, Younesid A, Amir N, Farahanie A, Mousazadeh M, Soleimanie P (2019) Performance of modified one-stage Phoredox reactor with hydraulic up-flow in biological removal of phosphorus from municipal wastewater. Desalin Water Treat 171:216–222. https://doi.org/10.5004/dwt.2019.24752

Jose S, Mishra L, Debnath S, Pal S, Munda PK, Basu G (2019) Improvement of water quality of remnant from chemical retting of coconut fibre through electrocoagulation and activated carbon treatment. J Clean Prod 210:630–637. https://doi.org/10.1016/j.jclepro.2018.11.011

Kékedy-Nagy L, Moore JP, Abolhassani M, Attarzadeh F, Hestekin JA, Greenlee LF (2019) The passivating layer influence on Mg-based anode corrosion and implications for electrochemical struvite precipitation. J Electrochem Soc 166(12):E358. https://doi.org/10.1149/2.0901912jes

Kékedy-Nagy L, Abolhassani M, Perez Bakovic SI, Anari Z, Moore JP II, Pollet BG, Greenlee LF (2020) Electroless production of fertilizer (struvite) and hydrogen from synthetic agricultural wastewaters. J Am Chem Soc 142:18844–18858. https://doi.org/10.1021/jacs.0c07916

Kim JH, An BM, Lim DH, Park JY (2018) Electricity production and phosphorous recovery as struvite from synthetic wastewater using magnesium-air fuel cell electrocoagulation. Water Res 132:200–210. https://doi.org/10.1016/j.watres.2018.01.003

Krishnamoorthy N, Dey B, Arunachalam T, Paramasivan B (2020) Effect of storage on physicochemical characteristics of urine for phosphate and ammonium recovery as struvite. Int Biodeterior Biodegrad 153:105053. https://doi.org/10.1016/j.ibiod.2020.105053

Krishnamoorthy N, Dey B, Unpaprom Y, Ramaraj R, Maniam GP, Govindan N, Jayaraman S, Arunachalam T, Paramasivan B (2021) Engineering principles and process designs for phosphorus recovery as struvite: a comprehensive review. J Environ Chem Eng 9(5):105579. https://doi.org/10.1016/j.jece.2021.105579

Kruk DJ, Elektorowicz M, Oleszkiewicz JA (2014) Struvite precipitation and phosphorus removal using magnesium sacrificial anode. Chemosphere 101:28–33. https://doi.org/10.1016/j.chemosphere.2013.12.036

Kurtulus G, Tas AC (2011) Transformations of neat and heated struvite ($MgNH_4PO_4{\cdot}6H_2O$). Mater Lett 65:2883–2886. https://doi.org/10.1016/j.matlet.2011.06.086

Lahr RH, Goetsch HE, Haig SJ, Noe-Hays A, Love NG, Aga DS, Bott CB, Foxman B, Jimenez J, Luo T, Nace K, Ramadugu K, Wigginton KR (2016) Urine bacterial community convergence through fertilizer production: storage, pasteurization, and struvite precipitation. Environ Sci Technol 50:11619–11626. https://doi.org/10.1021/acs.est.6b02094

Lee EY, Oh MH, Yang S-H, Yoon TH (2015) Struvite crystallization of anaerobic digestive fluid of swine manure containing highly concentrated nitrogen. Asian Australas J Anim Sci 28:1053. https://doi.org/10.5713/2Fajas.14.0679

Li S, Zeng W, Xu H, Jia Z, Peng Y (2020) Performance investigation of struvite high-efficiency precipitation from wastewater using silicon-doped magnesium oxide. Environ Sci Pollut Res 13:15463–15474. https://doi.org/10.1007/s11356-019-07589-3

Lin Q, Chen Z, Liu J, Tang B, Ye J, Zhang L (2015) Optimization of struvite crystallization to recover nutrients from raw swine wastewater. Desalin Water Treat 56:3106–3112. https://doi.org/10.1080/19443994.2014.963686

Lin X, Han Z, Yu H, Ye Z (2018) Struvite precipitation from biogas digestion slurry using a two-chamber electrolysis cell with a magnesium anode. J Clean Prod 174:1598–1607. https://doi.org/10.1016/j.jclepro.2017.10.224

Luo W, Fang Y, Song L, Niu Q (2022) Production of struvite by magnesium anode constant voltage electrolytic crystallisation from anaerobically digested chicken manure slurry. Environ Res 214:113991. https://doi.org/10.1016/j.envres.2022.113991

Mohora E, Rončević S, Dalmacija BŽ, Agbaba J, Watson M, Karlovic E, Dalmacija M (2012) Removal of natural organic matter and arsenic from water by electrocoagulation/flotation continuous flow reactor. J Hazard Mater 235–236:257–264. https://doi.org/10.1016/j.jhazmat.2012.07.056

Moradi M, Vasseghian Y, Arabzade H, Khaneghah AM (2021) Various wastewaters treatment by sono-electrocoagulation process: a comprehensive review of operational parameters and future outlook. Chemosphere 263:128314. https://doi.org/10.1016/j.chemosphere.2020.128314

Mores R, Treichel H, Zakrzevski CA, Kunz A, Steffens J, Dallago RM (2016) Remove of phosphorous and turbidity of swine wastewater using electrocoagulation under continuous flow. Sep Purif Technol 171:112–117. https://doi.org/10.1016/j.seppur.2016.07.016

Naghipour D, Rouhbakhsh E, Jaafari J (2020) Application of the biological reactor with fixed media (IFAS) for removal of organic matter and nutrients in small communities. Int J Environ Anal Chem 1-11. https://doi.org/10.1080/03067319.2020.1803851

Nageshwari K, Balasubramanian P (2022) Evolution of struvite research and the way forward in resource recovery of phosphates through scientometric analysis. J Clean Prod 357:131737. https://doi.org/10.1016/j.jclepro.2022.131737

Naje AS, Chelliapan S, Zakaria Z, Abbas SA (2016) Electrocoagulation using a rotated anode: A novel reactor design for textile wastewater treatment. J Environ Manag 176:34–44. https://doi.org/10.1016/j.jenvman.2016.03.034

Omwene PI, Kobya M (2018) Treatment of domestic wastewater phosphate by electrocoagulation using Fe and Al electrodes: a comparative study. Process Saf Environ Prot 116:34–51. https://doi.org/10.1016/j.psep.2018.01.005

Peng L, Dai H, Wu Y, Peng Y, Lu X (2018) A comprehensive review of the available media and approaches for phosphorus recovery from wastewater. Water Air Soil Pollut 229(4):1–28. https://doi.org/10.1007/s11270-018-3706-4

Pilarska AA, Klapiszewski Ł, Jesionowski T (2017) Recent development in the synthesis, modification and application of $Mg(OH)_2$ and MgO: a review. Powder Technol 319:373–407. https://doi.org/10.1016/j.powtec.2017.07.009

Rajaniemi K, Hu T, Nurmesniemi ET, Tuomikoski S, Lassi U (2021) Phosphate and ammonium removal from water through electrochemical and chemical precipitation of struvite. Processes 9(1):150. https://doi.org/10.3390/pr9010150

Sandoval MA, Espinoza LC, Coreño O, García V, Fuentes R, Thiam A, Salazar R (2022) A comparative study of anodic oxidation and electrocoagulation for treating cattle slaughterhouse wastewater. J Environ Chem Eng 10(5):108306. https://doi.org/10.1016/j.jece.2022.108306

Shahnaz T, S. MMF, V.C. P, Narayanasamy S (2020) Surface modification of nanocellulose using polypyrrole for the adsorptive removal of Congo red dye and chromium in binary mixture. Int J Biol Macromol 151:322–332. https://doi.org/10.1016/j.ijbiomac.2020.02.181

Shu J, Liu R, Liu Z, Chen H, Tao C (2016) Simultaneous removal of ammonia and manganese from electrolytic metal manganese residue leachate using phosphate salt. J Clean Prod 135:468–475. https://doi.org/10.1016/j.jclepro.2016.06.141

Siciliano A (2016) Assessment of fertilizer potential of the struvite produced from the treatment of methanogenic landfill leachate using low-cost reagents. Environ Sci Pollut Res 23:5949–5959. https://doi.org/10.1007/s11356-015-5846-z

Siciliano A, Limonti C, Curcio GM, Molinari R (2020) Advances in struvite precipitation technologies for nutrients removal and recovery from aqueous waste and wastewater. Sustainability 12(18):7538. https://doi.org/10.3390/su12187538

Song G (2005) Recent progress in corrosion and protection of magnesium alloys. Adv Eng Mater 7:563–586. https://doi.org/10.1002/adem.200500013

Suguna K, Thenmozhi M, Sekar C (2012) Growth, spectral, structural and mechanical properties of struvite crystal grown in presence of sodium fluoride. Bull Mater Sci 35(4):701–706

Tao W, Fattah KP, Huchzermeier MP (2016) Struvite recovery from anaerobically digested dairy manure: a review of application potential and hindrances. J Environ Manag 169:46–57. https://doi.org/10.1016/j.jenvman.2015.12.006

Tejera J, Hermosilla D, Gascó A, Miranda R, Alonso V, Negro C, Blanco Á (2021) Treatment of mature landfill leachate by electrocoagulation followed by Fenton or UVA-LED photo-Fenton processes. J Taiwan Inst Chem Eng 119:33–44. https://doi.org/10.1016/j.jtice.2021.02.018

Tian X, Wang G, Guan D, Li J, Wang A, Li J, Yu Z, Chen Y, Zhang Z (2016) Reverse osmosis brine for phosphorus recovery from source separated urine. Chemosphere 165:202–210. https://doi.org/10.1016/j.chemosphere.2016.09.037

Tibebe D, Kassa Y, Bhaskarwar AN (2019) Treatment and characterization of phosphorus from synthetic wastewater using aluminum plate electrodes in the electrocoagulation process. BMC Chem 13(1):1–4. https://doi.org/10.1186/s13065-019-0628-1

Thakur C (2021) Unification electrocoagulation-adsorption treatment for removal of COD and surfactant from automobile wastewater. Int J Chem React Eng 19(9):961–968. https://doi.org/10.1515/ijcre-2021-0095

Udert KM, Larsen TA, Gujer W (2003) Biologically induced precipitation in urine-collecting systems. Water Sci Technol Water Supply 3(3):71–78. https://doi.org/10.2166/ws.2003.0010

Udert KM, Larsen TA, Gujer W (2006) Fate of major compounds in source-separated urine. Water Sci Technol 54(11-12):413–420. https://doi.org/10.2166/wst.2006.921

Wang F, Fu R, Lv H, Zhu G, Lu B, Zhou Z, Wu X, Chen H (2019) Phosphate recovery from swine wastewater by a struvite precipitation electrolyzer. Scientific reports 9(1):1-0. https://doi.org/10.1038/s41598-019-45085-3

Yetilmezsoy K, Ilhan F, Kocak E, Akbin HM (2017) Feasibility of struvite recovery process for fertilizer industry: A study of financial and economic analysis. J Clean Prod 152:88–102. https://doi.org/10.1016/j.jclepro.2017.03.106

Zeng L, Li X (2006) Nutrient removal from anaerobically digested cattle manure by struvite precipitation. J Environ Eng Sci 5:285–294. https://doi.org/10.1139/S05-027

Zhang T, Wang Q, Deng Y, Jiang R (2018) Recovery of phosphorus from swine manure by ultrasound/H2O2 digestion, struvite crystallization, and ferric oxide hydrate/biochar adsorption. Front Chem 464. https://doi.org/10.3389/fchem.2018.00464

Zhang X, Lin H, Hu B (2016) Phosphorus removal and recovery from dairy manure by electrocoagulation. RSC Adv 6(63):57960–57968. https://doi.org/10.1039/C6RA06568F

Zhou X, Chen Y (2019) An integrated process for struvite electrochemical precipitation and ammonia oxidation of sludge alkaline hydrolysis supernatant. Environ Sci Pollut Res 26:2435–2444. https://doi.org/10.1007/s11356-018-3667-6

Publisher's note Springer Nature remains neutral with regard to jurisdictional claims in published maps and institutional affiliations.

Springer Nature or its licensor holds exclusive rights to this article under a publishing agreement with the author(s) or other rightsholder(s); author self-archiving of the accepted manuscript version of this article is solely governed by the terms of such publishing agreement and applicable law.